

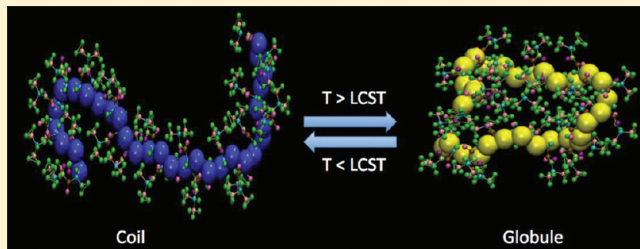
Role of Solvation Dynamics and Local Ordering of Water in Inducing Conformational Transitions in Poly(*N*-isopropylacrylamide) Oligomers through the LCST

Sanket A. Deshmukh,[†] Subramanian K. R. S. Sankaranarayanan,^{*,†} Kamlesh Suthar,[‡] and Derrick C. Mancini^{*,†,‡}

[†]Center for Nanoscale Materials and [‡]Advanced Photon Source, Argonne National Laboratory, Argonne, Illinois 60439, United States

 Supporting Information

ABSTRACT: Conformational transitions in thermo-sensitive polymers are critical in determining their functional properties. The atomistic origin of polymer collapse at the lower critical solution temperature (LCST) remains a fundamental and challenging problem in polymer science. Here, molecular dynamics simulations are used to establish the role of solvation dynamics and local ordering of water in inducing conformational transitions in isotactic-rich poly(*N*-isopropylacrylamide) (PNIPAM) oligomers when the temperature is changed through the LCST. Simulated atomic trajectories are used to identify stable conformations of the water-molecule network in the vicinity of polymer segments, as a function of the polymer chain length. The dynamics of the conformational evolution of the polymer chain within its surrounding water molecules is evaluated using various structural and dynamical correlation functions. Around the polymer, water forms cage-like structures with hydrogen bonds. Such structures form at temperatures both below and above the LCST. The structures formed at temperatures above LCST, however, are significantly different from those formed below LCST. Short oligomers consisting of 3, 5, and 10 monomer units (3-, 5-, and 10-mer), are characterized by significantly higher hydration level (water per monomer ~ 16). Increasing the temperature from 278 to 310 K does not perturb the structure of water around the short oligomers. In the case of 3-, 5-, and 10-mer, a distinct coil-to-globule transition was not observed when the temperature was raised from 278 to 310 K. For a PNIPAM polymer chain consisting of 30 monomeric units (30-mer), however, there exist significantly different conformations corresponding to two distinct temperature regimes. Below LCST, the water molecules in the first hydration layer (~ 12) around hydrophilic groups arrange themselves in a specific ordered manner by forming a hydrogen-bonded network with the polymer, resulting in a solvated polymer acting as hydrophilic. Above LCST, this arrangement of water is no longer stable, and the hydrophobic interactions become dominant, which contributes to the collapse of the polymer. Thus, this study provides atomic-scale insights into the role of solvation dynamics in inducing coil-to-globule phase transitions through the LCST for thermo-sensitive polymers like PNIPAM.



I. INTRODUCTION

Understanding the conformational transitions of single linear polymer chains is a fundamental problem in the field of polymer science.^{1–5} These conformational changes can be brought about by altering environmental variables such as temperature, or pH, or light, or by providing external stimuli such as magnetic and electric fields.⁶ Thermo-sensitive polymers such as poly(*n*-isopropylacrylamide) (PNIPAM) represent an important class of materials that undergo a coil-to-globule transition as the temperature is raised through the LCST, which is around 305 K for atactic PNIPAM.^{7–9} These coil-to-globule transitions are important in a number of practical applications, including drug delivery, medical diagnostics, tissue engineering, electrophoresis, separation, and enhanced oil recovery.^{10–14} For example, tuning the LCST of PNIPAM to be close to the human body temperature by copolymerization could enable development of controlled drug delivery systems.^{15–17}

Several recent experiments have attempted to study the nature of these conformational transitions through the LCST.^{9,18–20} While there has been much effort devoted to the static properties of short polymer chains, much less is understood about polymer dynamics in these systems.^{21,22} Little is known about the effect of the local structure of the surrounding solvent and its interactions with the polymer on the conformational transitions.²³ In particular, little is known about the role of proximal water molecules and their solvation dynamics in inducing conformational phase transitions through the LCST.^{24–28} Limited experimental and theoretical work has focused on investigating the effect of fluid–polymer interactions on the static and dynamic properties, or on the local molecular perturbation of the water structure and polymer conformation on the resulting

Received: November 9, 2011

Revised: January 30, 2012

Published: February 2, 2012

molecular architecture.^{23–27,29–37} Specifically, the molecular sequence of steps leading to the collapse of the short oligomers is not yet understood. Atomic-scale insights into the precise mechanism of these conformational transitions would be critical to exercising control over the structure and transport properties of polymers.

In this work, we study the solvation of PNIPAM in water in order to gain atomistic insights into the nature of the conformational transformation of a model thermo-sensitive polymer. Below the LCST of 305 K, PNIPAM is soluble in water, and above 305 K it becomes hydrophobic.¹⁹ The origin of this hydrophilic-to-hydrophobic transition, as well as the molecular changes in the solvation dynamics and structure of water during and after this transition, are not well understood. Moreover, the size dependence of this coil-to-globule transition in the case of short oligomers is still unknown.

Several theories have been proposed to explain this coil-to-globule transition at LCST.^{38–40} One thermodynamic theory suggests that this transition is the result of the entropic gain in the “somewhat arranged” water molecules near the hydrophobic group(s) above the LCST.¹⁹ Once this entropy term dominates the enthalpy of hydrogen bonds between PNIPAM polar groups and water molecules, PNIPAM is more stable in globular conformation. In the case of oligomers of PNIPAM, however, the LCST behavior is the result of the intramolecular aggregation at elevated temperature.^{22,23} Another study, by Ahmed et al., has proposed the existence of a characteristic length scale, termed “persistent length”, for cross-linked PNIPAM hydrogel nanoparticles to show any kind of volume phase transition (VPT) behavior.⁴¹ At lengths shorter than the persistent length, the polymer acts like an “elastic rod”, whereas at lengths longer than the persistent length the polymer backbone conformation forms a random coil. This study by Ahmed et al. emphasizes that both polymer–water and polymer–polymer interactions play a key role in determining the VPT and the LCST of PNIPAM.

Similarly, there have been several molecular dynamics (MD) simulation studies on understanding the conformational transformations in PNIPAM oligomers.^{23,29,42,43} Longhi et al. have carried out MD simulations of PNIPAM oligomers consisting of 50 monomer units at 300 K and at 310 K (namely, below and above the LCST of PNIPAM).³⁷ They observed a coil-to-globule transition of PNIPAM above the LCST and also found that water organizes itself differently close to and away from the oligomer. Gangemi et al. further extended the study carried out by Longhi et al. by increasing the simulation length and by studying PNIPAM oligomer as well as two oligomers of PNIPAM having N-methacryloyl-L-valine and N-methacryloyl-L-leucine comonomers.³⁶ Gangemi et al. carried out simulations of PNIPAM oligomer with 26 monomer units for 75 ns at 302 and 315 K. They observed a clear coil-to-globule transition of PNIPAM and its co-oligomers at 315 K. Recently, Du et al. have studied the effect of salt ions on the LCST of PNIPAM.²⁹ In their study, they carried out simulations of PNIPAM in 1 M of NaCl, NaBr, NaI, and KCl to elucidate the effects of different salt ions on the LCST of PNIPAM. Du et al. found that cations have a much stronger affinity with the polymer, whereas anions bind weakly with the polymer.²⁹ In another study, Du et al. carried out MD simulations of copolymer of PNIPAM (38 monomer units) and poly(ethylene glycol) methacrylate (PEGMA) (2 monomer units) copolymer in NaCl solution.⁴³ The PNIPAM-*co*-PEGMA was observed to go through the hydrophilic–hydrophobic conformational change for simulations at temperature slightly above its LCST. They found that Na⁺ ions bind strongly and directly with

amide O, and even more strongly with the O atoms on PEGAMS chains, whereas Cl[−] ions only exhibit weak interaction with the polymer.

The LCST of PNIPAM is also affected by its tacticity.⁴⁴ An increase in the isotacticity of the PNIPAM chain decreases the LCST of PNIPAM.⁴⁴ Ray et al. reported experimentally that the LCST of PNIPAM increases from ~17.0 to 29.5 °C with a decrease in the isotactic content from 66% to 51%.⁴⁴ In the present work, the 30-mer chains have a meso (*m*) diad content of ~57% and hence are expected to have an LCST of ~301 K. It has also been suggested by Ray et al. that the hydrogen bonding between the amide groups and hydrophobic bonding among isopropyl moieties of side groups of PNIPAM might become stronger with an increase in the isotacticity, and the hydrogen bonding between the amide groups and water molecules might become weaker at the cost of the formation of the hydrogen bond between the amide groups. This could explain the lowering of LCST in the case of isotactic polymer chains.⁴⁴

Recent experimental investigations suggest that the LCST is strongly correlated to the solvation behavior of the polymer.^{3,45–49} Ono and Shikata used high-frequency dielectric relaxation techniques to study the hydration of PNIPAM in water.^{25,26} They attribute the temperature-induced phase transition to the dehydration of PNIPAM above the LCST. This suggests that above the LCST, both the PNIPAM conformational structure and the structure of water near the polymer are different from that below the LCST. Therefore, water plays a critical role in determining the LCST of PNIPAM.

Several fundamental questions remain unanswered regarding the role of the local structure of water and solvation dynamics in influencing the LCST. For example, what is the effect of the local structure of the surrounding solvent and its interactions with the polymer on the conformational transitions for the short oligomers? The exact atomic-level orientation of water molecules near hydrophilic and hydrophobic groups is not understood, and neither is the role and network of the bridged water molecules between monomer units. Also unclear is the stability of the ordered solvation structure and the interplay between the exchange kinetics of proximal water and the level of hydration of the polymer. Finally, the relationship of the conformational transitions to the polymer chain size has not been studied.

Here, we employ MD simulations to understand the detailed mechanism behind the size-dependent coil-to-globule transition of PNIPAM above the LCST. Simulations of oligomers of PNIPAM ranging from 3 to 30-mers were carried out at temperatures below and above the LCST, namely at 278 and 310 K. Dynamical correlation functions, such as radius of gyration (R_g) and radial distribution function (RDF) computed from the simulated atomic trajectories are utilized to identify the nature of conformational transitions near LCST. The structure of water in proximity to the polymer structure, for temperatures both below and above the LCST, was evaluated in terms of hydrogen bonding characteristics between the polymer and itself, between polymer and water, and between water and water. Residence probability of water molecules near the polymer was calculated to understand the exchange kinetics and strength of polymer–water interactions. The atomic trajectories are used to identify the formation and evolution of the solvation cage and the local structure of water, below and above the LCST. Where possible, simulation results are compared with available experimental studies.

II. COMPUTATIONAL DETAILS

a. Potential Model. To study the coil-to-globule transition in PNIPAM, we have used a fully atomistic model of PNIPAM and water. Choice of a suitable force-field determines the accuracy of the MD simulations. Polymer consistent force-field (PCFF) has been successfully used in the past to carry out MD simulation of different polymers.^{50–54} In this work, we have used a PCFF force-field, with its form given by eq 1.^{50,51}

$$\begin{aligned}
 E_{pot} = & \sum_b [K_2(b - b_0)^2 + K_3(b - b_0)^4 + K_4(b - b_0)^4] \\
 & + \sum_\theta H_2(\theta - \theta_0)^2 + H_3(\theta - \theta_0)^3 + H_4(\theta - \theta_0)^4 \\
 & + \sum_\varphi [V_1[1 - \cos(\varphi - \varphi_1^0)] + V_2[1 - \cos(2\varphi - \varphi_2^0)] \\
 & \quad + V_3[1 - \cos(3\varphi - \varphi_3^0)]] \\
 & + \sum_x K_x x^2 + \sum_b \sum_{b'} F_{bb'}(b - b_0)(b' - b'_0) \\
 & + \sum_\theta \sum_{\theta'} F_{\theta\theta}(\theta - \theta_0)(\theta' - \theta'_0) \\
 & + \sum_b \sum_{\theta} F_{b\theta}(b - b_0)(\theta - \theta_0) \\
 & + \sum_b \sum_{\varphi} (b - b_0)[V_1 \cos \varphi + V_2 \cos 2\varphi + V_3 \cos 3\varphi] \\
 & + \sum_{b'} \sum_{\varphi} (b' - b'_0)[V_1 \cos \varphi + V_2 \cos 2\varphi + V_3 \cos 3\varphi] \\
 & + \sum_\theta \sum_{\varphi} (\theta - \theta_0)[V_1 \cos \varphi + V_2 \cos 2\varphi + V_3 \cos 3\varphi] \\
 & + \sum_\varphi \sum_{\theta} \sum_{\theta'} K_{\varphi\theta\theta'} \cos \varphi (\theta - \theta_0)(\theta' - \theta'_0) \\
 & + \sum_{i>j} q_i q_j \frac{1}{\epsilon r_{ij}} + \sum_{i>j} [(A_{ij}/r_{ij}^9) - (B_{ij}/r_{ij}^6)]
 \end{aligned}
 \quad (1)$$

In eq 1, terms (1), (2), (3), and (4) are the bond stretching, angle bending, dihedral, and the out-of-plane (also called inversion) terms, respectively. Term b_0 is the equilibrated bond length of the bond, b is the bond length during simulations, and K_2 , K_3 , and K_4 are the corresponding force constants. θ_0 and θ are the equilibrium angle and observed angle during simulations, respectively, and H_2 , H_3 , and H_4 are the corresponding force constants. Similarly, φ_0 and φ are the equilibrium dihedral angle and dihedral angle during the simulations, respectively, and V_1 , V_2 , and V_3 are corresponding force constants. χ is the out-of-plane angle and K_χ is the corresponding force constant. Terms (5) to (11) define the cross interactions, which include the dynamic variations among the bond stretching, bending, and torsion angle rotation. $F_{bb'}$ is the force constant for the cross term between two bonds with one common atom, $F_{\theta\theta}$ refers to the force constant for the two angles (θ and θ') with a common bond, and $F_{b\theta}$ is the force constant for the cross term between a bond and an angle in which the bond is one of the edges. The last two terms, (12) and (13), describe the Coulombic electrostatic force and Van-der Waals interactions, respectively. r_{ij} is the distance between two atoms i and j . ϵ is the dielectric constant and q_i and q_j are the charges on atoms i and j . Numerical values of the various force-field parameters are available in refs 55 and 56. A PCFF water model, with partial charge of -0.798 on oxygen atom and $+0.399$ on hydrogen atom,

was used in all the simulations (see Supporting Information, Table S1).^{54,57} Figure 1 shows the partial charges used by PCFF force-field to represent the PNIPAM polymer.

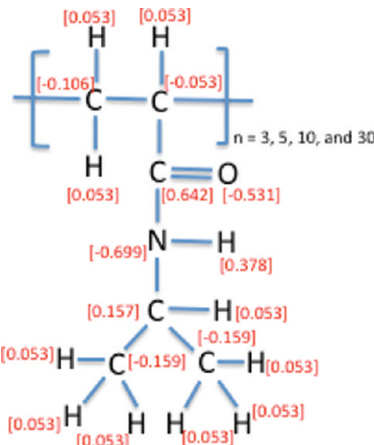


Figure 1. Partial charges (e) [in red] and atom types for PNIPAM.

b. MD Simulation Details. Fully atomistic models of PNIPAM chains consisting of 3, 5, 10, and 30-mers were placed in a cubic simulation cell which was subsequently filled with water molecules (PCFF water model). In the first step of the structure generation, a monomer unit (shown in Figure 1) was generated and placed in a simulation cell. The second monomer was placed at a bond-distance (between backbone atoms) of ~ 1.55 Å from the first monomer. In other words, based on the distance defined by the PCFF force-field, the distance between carbon atom of $-\text{CH}_2-$ group of the first monomer and the carbon atom of $-\text{CH}-$ group of the second monomer was chosen to be ~ 1.55 Å. The rotational state of this second monomer was chosen randomly. The length of the backbone chain was increased progressively along the x -direction by adding subsequent monomer units whose backbone atoms were placed at ~ 1.55 Å from the adjacent monomer. This process was continued until desired numbers of monomer units were added to form PNIPAM oligomers (with 5, 10, and 30 monomer units). The tacticity of each of these generated polymer chains was computed by identifying the percentage of meso (m) diads in the generated oligomers. The tacticity varied from 57% for 30-mer to 66% for 5-mer. The 3-mer chain was isotactic with $m = 100$. Thus, all chains were isotactic-rich. Once this initial polymer structure is generated, the next step is the equilibration of the polymer chains. These chains were initially equilibrated for 100 ps. Following this relaxation, PCFF water molecules were inserted randomly. The initial water density was chosen to be close to bulk water ~ 1 g/cm³. The simulations were then carried out for a total of 20 ns, of which 18 ns were considered as the production run. The equilibration of system temperature, density, and total energy was attained within the initial 2 ns of the simulation run. Additionally, based on the root-mean-square displacement (rmsd) of PNIPAM oligomer chains, we find that structural equilibration was attained within initial 5 ns of simulation run. Hence, atomic trajectories of last 5 to 10 ns were considered for all the dynamical analysis. Systems studied are listed in Table 1.

To study the structural evolution of polymer and water above the LCST, simulations were conducted in *NPT* (moles (N), pressure (P), and temperature (T) are conserved) ensemble at 278 and 310 K at 1 atm pressure. Nose–Hoover thermostat and barostat were used to maintain the temperature and

Table 1. System Details Employed in This Study

system	no. of PNIPAM monomers	no. of waters	density (gm/cm ³) (after the relaxation of 2 ns)	% of meso (<i>m</i>) diad
A	3	1000	1.013	100
B	5	1200	1.026	~66
C	10	3000	1.027	~62
D	30	9000	1.025	~57

pressure with time constants of 1 and 2 ps, respectively.⁵⁸ The LAMMPS simulation package was used to carry out all the simulations with periodic boundary conditions.⁵⁹ A spherical cutoff of 9.5 Å was used for all nonbonded interactions. The Ewald summation method was used to calculate the long-ranged electrostatic interactions. Simulations were carried out for 20 ns with a time step of 1 fs. The atomic trajectories (atom positions, temperature, pressure, velocities etc.) were accumulated and stored every 1 ps. Trajectory files obtained from these simulations were analyzed for various structural and dynamical properties.

Radial distribution functions (RDFs) were calculated to determine the difference in the structural arrangements of polymer and water below and above the LCST. The calculations were performed on the key atom pairs involved in hydrogen bonding namely, carbonyl oxygen (op) and hydrogen (hw) of water to evaluate the effect of temperature. RDF for the carbon atom of PNIPAM backbone (ch2b) with water oxygen (ow) was also calculated.

The structural evolution was followed by analyzing the change in R_g over time. The instantaneous R_g which is a measure of the size of a group of oligomer, was calculated for each frame of atomic trajectory using eq 2.

$$R_g^2 = \frac{1}{M} \sum_i m_i (r_i - r_{cm})^2 \quad (2)$$

where M is the mass of the group, r_{cm} is the center of mass position of the group, and the sum is over all the atoms in the group.

Residence probability of water in the first hydration shell of polymer, $P_{\text{res}}(t)$, was calculated for water molecules both below and above the LCST, namely at 278 and 310 K. Water molecules were divided into three different regions:

- (1) hydrophilic (water molecules located in the region that covers the inner part up to the first peak in the RDF of water oxygen atoms and hydrophilic atoms of polymer ($-N-H$) and ($C=O$)))
- (2) hydrophobic (water molecules located in the region that covers the inner part up to the first peaks of RDF of water oxygen atoms and hydrophobic atoms of polymer (backbone of polymer and isopropyl moieties in the side-group))
- (3) bulk water (water molecules located in the region that extends beyond the first peak in RDFs of the water oxygen atoms and the hydrophilic/hydrophobic atoms).

$P_{\text{res}}(t)$ was defined, by continuous definition, as the probability of finding a water molecule in one of the above-defined regions without departing from that region at any time between time t_0 and $t + t_0$. $P_{\text{res}}(t)$ was averaged over 10 000 different simulation frames which were collected over a time frame of 100 ps in intervals of 0.01 ps. In the case of the residence probability of water molecules defined by the intermittent definition, the molecules residing initially at t_0 are also taken into account for

the residence correlation at time $t_0 + t$ even if they have departed from that region in the time interval between t_0 and $t_0 + t$.

Prior studies suggest that water-polymer interactions play a very important role in coil-to-globule transition of PNIPAM.^{3,9,18,21,46,48} Hydrogen bonding is one major possible interaction. We have therefore studied the hydrogen bonding characteristics of water and polymer, which represents one of the major possible interactions between water and polymer. Effects of temperature and polymer chain length on the hydrogen bonding abilities of water with PNIPAM were assessed. The following geometric criteria were used to represent hydrogen bonding between a pair of water molecules:^{32,60}

$$\begin{aligned} R_{OO} &\leq 3.6 \text{ \AA} \\ R_{OH} &\leq 2.45 \text{ \AA} \\ \varphi &\leq 30^\circ \end{aligned} \quad (3)$$

In the above equations, R_{OO} represents the distance between oxygen and oxygen atoms of water 1 and 2. R_{OH} is the distance between oxygen atom and hydrogen atom of water 1 and water 2, respectively, which form the hydrogen bond. The angle φ is the angle between oxygen atom of water 1 and oxygen and hydrogen atoms of water 2 ($O_1 \cdots O_2-H_2$). In this study, the first minimum in the corresponding RDFs of pure water was chosen as the cutoff distances, R_{OO} and R_{OH} . A hydrogen bond defined by using these geometric criteria fulfills the potential energy requirements typical for hydrogen bonds in water.

Two types of hydrogen bonds are possible between polymer and water: (1) a bond between carbonyl oxygen (op) and water hydrogen (hw) and (2) a bond between hydrogen of amide group (hp) and water oxygen (ow). Similar to the criteria defined previously in the case of hydrogen bonds in water, we can define the geometric criteria for hydrogen bonds to exist between polymer and polymer, between polymer and water, and between water and polymer. In each of these cases, the distance criteria between the donor and acceptor atoms were assigned based on the location of the first peak of the RDF for respective donor and acceptor atoms. For example, to identify the hydrogen bonds between polymer and water, where polymer is donor [amide group of PNIPAM (np-hp)] and water [oxygen of water (ow)] is acceptor, the first distance criterion (R_{np-ow}) requires the distance between np atom of PNIPAM and oxygen atom of water (ow) to be ≤ 4.2 Å (based on the RDF of ow and np). The second distance criterion (R_{ow-hp}) requires the distance between acceptor (ow) and hydrogen (hp) atom to be ≤ 2.45 Å (based on the RDF of ow-hp) and the angle between acceptor-donor-hydrogen (ow-np-hw) atom is required to be $< 30^\circ$.

A hydrogen bond occupation number (S_{ij}) can distinguish between the hydrogen bonded and non-hydrogen bonded atoms.

$$\begin{aligned} \text{hydrogen bond occupation number } (S_{ij}) \\ = \begin{cases} 1 & (\text{hydrogen bonded}) \\ 0 & (\text{non-hydrogen bonded}) \end{cases} \end{aligned}$$

The stability of the hydrogen bonds was determined by defining a time-dependent autocorrelation function of this state variable S_{ij} that describes the existence or nonexistence of bonds between a selected donor-acceptor pair ij (eq 4). Two types of correlation functions can be defined: intermittent and continuous.^{61,62} In the case of continuous correlation, the hydrogen bond occupation number (S_{ij}) was allowed only one

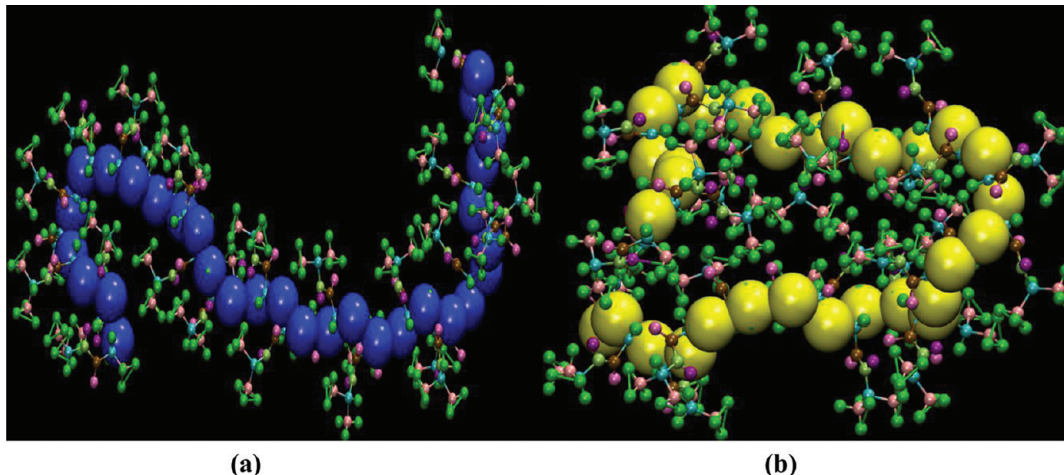


Figure 2. Snapshot of PNIPAM polymer chains for 30-mer taken at the end of a 20 ns of simulation at two temperatures: (a) 278 K (backbone carbon atoms of CH_2 are shown in blue) and (b) 310 K (backbone carbon atoms of CH_2 are shown in yellow). Water molecules have been omitted for clarity.

transition from 1 to 0 when the bond between atom i and j breaks for the first time. After the first breakage of hydrogen bonds between atom i and j , S_{ij} was never allowed to return to 1. In the case of intermittent correlation, $S_{ij}(t + t_0)$ was set to 1, if the bond between atom i and j was found to be present in the time steps t_0 and $t_0 + t$, irrespective of whether it is broken or reformed at intermediate times.

$$C_x(t) = \left\langle \frac{\sum_{ij} S_{ij}(t + t_0) \cdot S_{ij}(t_0)}{\sum_{ij} S_{ij}(t_0) \cdot S_{ij}(t_0)} \right\rangle \quad (4)$$

where x = continuous (c) or intermittent (i) autocorrelation function.

III. RESULTS AND DISCUSSION

A. Structural Analysis of Polymer.

tional Change. Figure 2 shows the structure of PNIPAM 30-mer after 20 ns of simulation time, below and above the LCST. Figure 2a shows that the polymer is in a coil state at 278 K at the end of 20 ns. It is clear from parts a and b of Figure 2 that the polymer has undergone a coil-to-globule transition as the temperature is increased from 278 to 310 K.

b. Radius of Gyration (R_g) and Radial Distribution Function (RDF). The extent and nature of the structural change for PNIPAM oligomers comprising 3-, 5-, 10-, and 30-mers is shown in terms of R_g and RDF in Figure 3a-d and in Figure 4a,b, respectively. R_g at 278 and 310 K, for PNIPAM with 3-, 5-, 10-, and 30-mer is shown in Figure 3, parts a-d, respectively. We find that R_g for short oligomers of PNIPAM such as 3-, 5-, and 10-mer indicates that the chain length of the polymer fluctuates around the respective mean value of R_g . This behavior is seen at both 278 and 310 K. For each of these short oligomers, the mean value of the R_g is shown in Table 2. We list the mean values of R_g and the standard deviation for the different chains at both the temperatures, i.e., 278 and 310 K. For each of these short oligomers such as 3-, 5-, and 10-mer, the mean value of the R_g is approximately equal at both the simulated temperatures, i.e., at 278 K and at 310 K.

We find, for example, that the R_g for 3-mer has a mean value of $R_g \sim 4.5$ Å at both 278 and 310 K whereas the deviation is ~ 0.2 . On the other hand, R_g for 5-mer and 10-mer show deviation in the mean R_g to be ~ 0.2 and ~ 0.3 at 278 K, respectively. Analysis

of the simulation trajectories suggests that, for 3, 5, and 10-mer, there is no clear distinction between an expanded or coil-like state and a collapsed or globule-like state at both 278 and 310 K. This observation is in excellent agreement with the recent experimental studies of Ahmed et al. They utilized dynamic light scattering, as well as steady state and time-resolved UV resonance Raman, to determine the change in the molecular conformations of the PNIPAM through the LCST.⁴¹ On the basis of their spectroscopic data, they suggested that short oligomers such as 3-mer to 10-mer might behave like an “elastic rod” and explores both the coil and globule conformations with equal probability.⁴¹

In Figure 3d, we present the R_g variation at 278 and 310 K for PNIPAM with degree of polymerization ~ 30 . Here, we find that there exists a clear difference in the temporal evolution of R_g at 278 and 310 K which indicates a clear coil-to-globule phase transition in PNIPAM above LCST (at 310 K).

As mentioned earlier, our aim is to investigate the atomic scale structural changes of water molecules near the polymer and their influence on the LCST. The RDF can be used to probe the local ordering of water molecules located close to the polymer. Toward this end, we calculate the RDF for hydrogen of water (h_w) with carbonyl oxygen (o_p) on the side chain and also for oxygen of water (o_w) and the carbon atom (ch_{2b}) of CH_2 group in the polymer backbone.

Parts a and b of Figure 4 show the RDF for PNIPAM carbonyl oxygen (op) on the side chain with hydrogen of water (hw) for 5 and 30-mer at 278 and 310 K, respectively. The RDF shows well-defined first and second neighbor peaks located at ~ 1.95 Å and ~ 3.18 Å, respectively. The peaks in the RDF indicate short-range structure through positional correlation. This correlation between the polymer and water molecules decreases with an increase in the temperature. This decrease in the short-range structural correlation is much more prominent in the case of 30-mer as compared to 5-mer. Positions of both first and second peaks are similar for both 5-mer and 30-mer at 278 and 310 K. However, the difference in the peak height of 30-mer indicates that the structure of water near polymer might be different at these two temperatures. The decrease in the height of the first and second neighbor peak correlates with the chain collapse (which is evident from Figure 3d) and suggests that the water is expelled from the

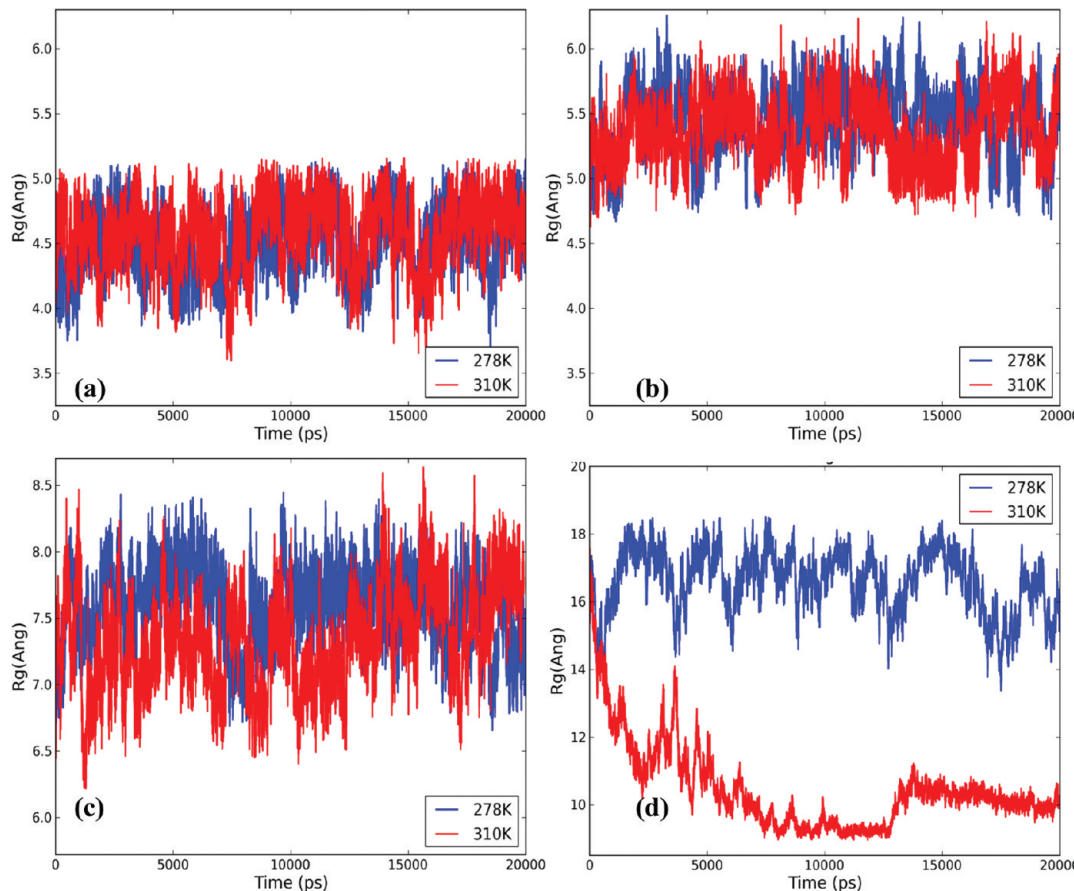


Figure 3. Radius of gyration (R_g) of PNIPAM polymer chains consisting of (a) 3-, (b) 5-, (c) 10-, and (d) 30-mers at 278 and 310 K.

center of the compact globule. This is also evident from the snapshots shown in Figure 2.

Parts c and d of Figures 4 show the RDF calculations for carbon atom of CH_2 of PNIPAM (ch2b) backbone with water oxygen (ow) at both 278 and 310 K. It can be seen from Figure 4c that, for 5-mer, there is no significant change in the positions of the first as well as second peaks at 278 and 310 K. This shows that, in the case of 5-mer, polymer–water positional correlations are similar both below and above the LCST of PNIPAM. As shown in Figure 4d, for 30-mer, there is a significant decrease in the peak intensity of the first peak at 310 K compared to 278 K. Additionally, the second peak is absent at 310 K which indicates that ordering of water in the second hydration shell near the polymer is significantly reduced above the LCST (at 310 K). Detailed analysis of the structural transformation of water molecules is presented in the subsequent sections.

B. Solvation Dynamics and Structural Evolution of Water Molecules. *a. Hydrogen Bonding Network.* The nature of hydrogen bonding of water molecules in the first few hydration shells near the polymer, below and above LCST, is still a subject of investigation and debate. Here, we use simulated trajectories and apply the geometric criteria defined earlier to establish the nature of the hydrogen bonding network in water (shown in green in Figure 5 and Figure 6) as the polymer chain undergoes a phase transformation. Figures 5 and 6 show the PNIPAM (30-mer) and hydrogen bonding network in water structures after simulating the structures for 20 ns at 278 and 310 K, respectively. The simulation snapshots can be used to evaluate the differences in the hydrogen bond network between water and water at 278 and 310 K. It should be noted that the

water molecules located near the hydrophobic groups of polymer cannot form hydrogen bonds with those hydrophobic groups. We observe that they have rearranged themselves to form a cage-like structure around the polymer, as shown in the zoomed-in view in Figure 5b.

Hydrogen bonds formed between water and polymer and between water and water both play a very important role in keeping the polymer hydrophilic.⁶³ Figure 6a shows the initial conformation of PNIPAM in water at 310 K. For simulation times <100 ps, the hydrogen bonding network in the water molecules appears similar to the final conformation at 278 K as shown in Figure 5a. Above the LCST, as shown in Figure 6b, the hydrogen bonds between water and polymer and between the cages of water are deformed, which makes the polymer hydrophobic. Parts c and d of Figure 6 show the PNIPAM structure at 310 K at the end of 12 and 20 ns, respectively. Note that this coil-to-globule transformation for 30-mer, seen in Figure 3d, is complete around ~3 ns and stays in globule form until 20 ns.

b. Extent of Hydration of Polymer Chains. To quantify the extent of the hydration behavior and changes in the structure of water cage, we calculated the number of water molecules in the first hydration shell (distance covering the inner region of the RDF of the oxygen of water and respective, hydrophilic or hydrophobic, group). The analysis was carried out for PNIPAM 3-, 5-, 10-, and 30-mer at 278 and 310 K. The results are summarized in Table 3 and the graphs are shown in Figure 7. It can be clearly seen that the extent of hydration of polymer chains decreases with the increase in polymer chain length. The average number of water molecules per CH_3 group in the first hydration shell in the case of 3-mer before undergoing LCST

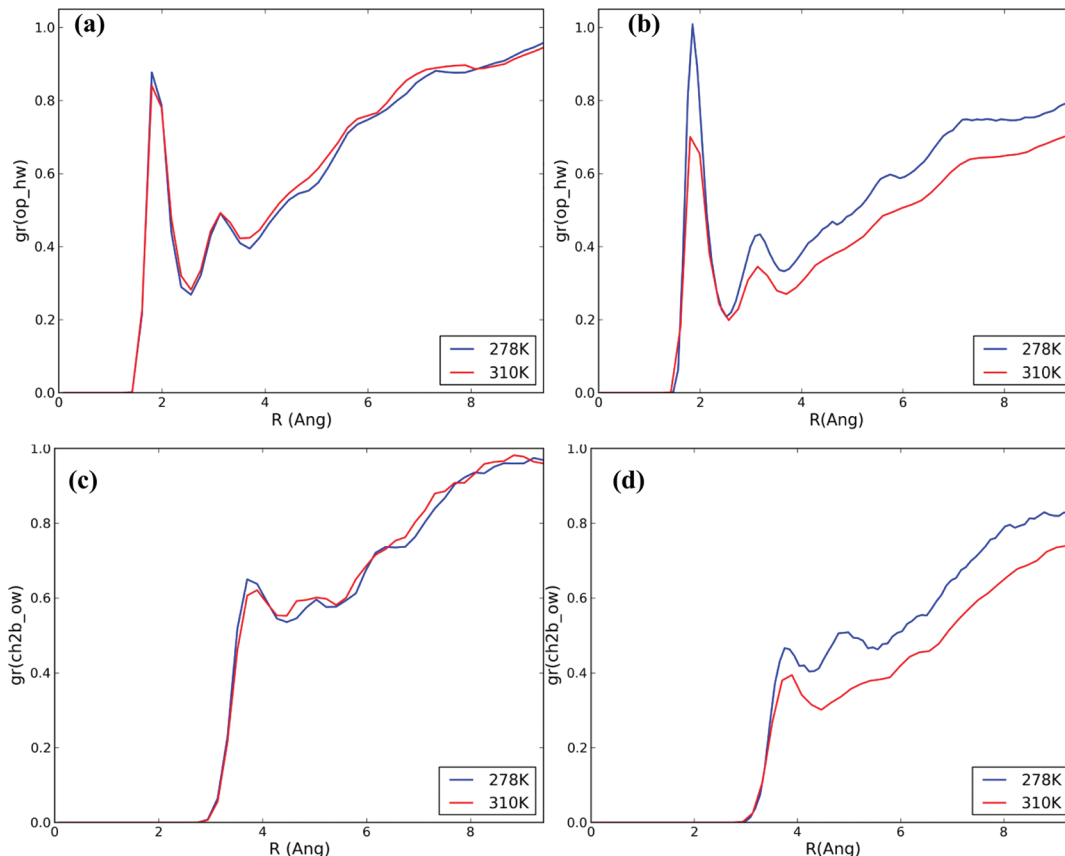


Figure 4. Radial distribution function (RDF) of carbonyl oxygen of polymer side chain (op) to water hydrogen (hw) at both 278 and 310 K is shown for (a) 5-mer (b) 30-mer. The RDF for carbon atom of CH_2 of PNIPAM backbone (ch2b) and water oxygen (ow) at both 278 and 310 K is shown for (c) 5-mer and (d) 30-mer.

Table 2. Mean value of R_g and standard deviation for the systems studied

	278 K		310 K	
	R_g (Å)	standard deviation	R_g (Å)	standard deviation
3-mer	4.5	0.2	4.8	0.2
5-mer	5.5	0.2	5.4	0.3
10-mer	7.6	0.3	7.3	0.4
30-mer	16.6	0.9	10.2	0.8

transition is ~ 8.6 , whereas the same in the case of 30-mer is ~ 5.9 . After the LCST transition, the average number of water

molecules per CH_3 is ~ 8.1 for 3-mer and ~ 3.8 for 30-mer. Similarly, the average number of water molecules per hydrophilic group at 278 K changes from ~ 3.0 for 3-mer to ~ 1.9 for 30-mer. At the two simulated temperatures (i.e., 278 and 310 K), we find that for short oligomers of PNIPAM, namely 3-, 5-, and 10-mer, there is no significant difference ($<10\%$) in the number of water molecules in the first hydration shell near both hydrophilic and hydrophobic groups. We did not observe any structural difference in polymers with 3-, 5-, and 10-mer, above and below the LCST of PNIPAM. This suggests that the hydrophilic interactions are dominant in these

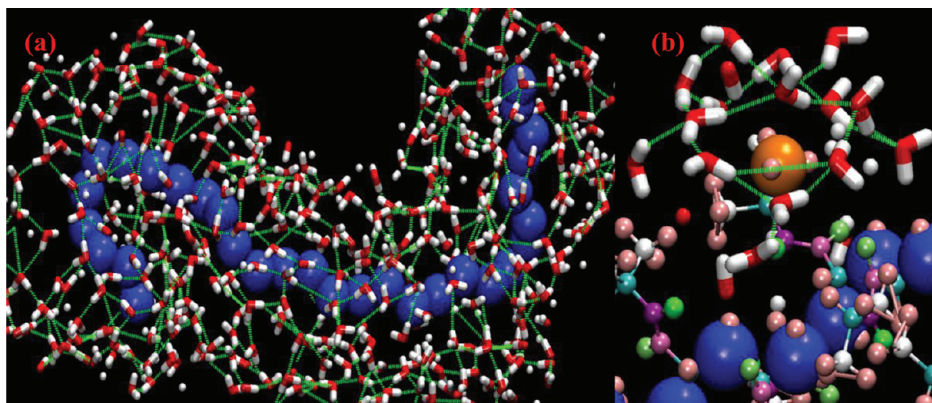


Figure 5. Hydrogen bond network, shown in green color, in water near polymer at 278 K after 20 ns (a) polymer chain backbone atoms shown in blue (b) CH_3 group (shown in orange color) surrounded by water molecules.

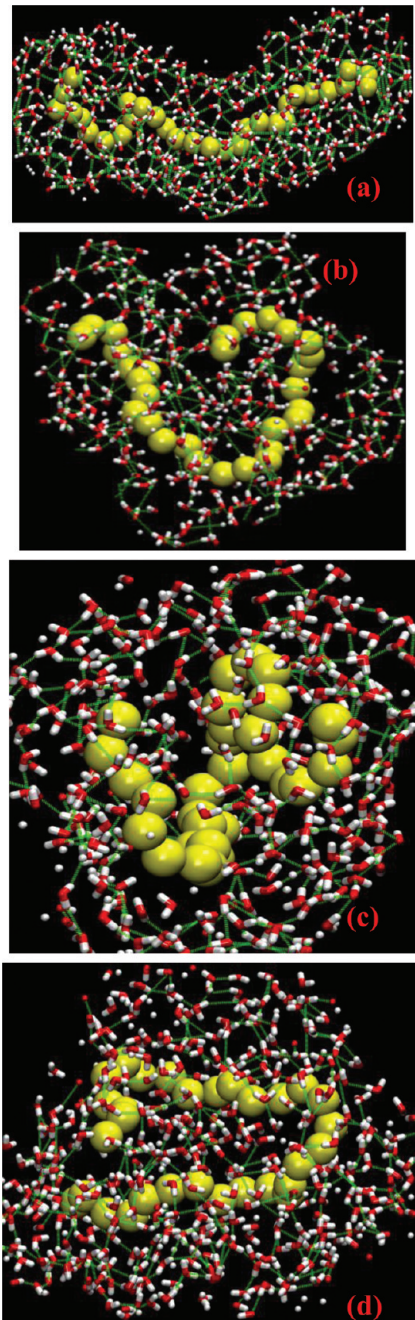


Figure 6. Hydrogen bond network in water at 310 K (a) after 0.002 ps and (b) after 6 ns (c) after 12 ns and (d) after 20 ns.

short oligomers and prevent them from undergoing a hydrophobic collapse within the simulated temperature range.

We now analyze closely the change in hydration behavior of 30-mer which does undergo a coil-to-globule transformation. At 278 K, i.e., below the LCST of PNIPAM, 30-mer has on an average ~ 12 water molecules per monomer unit. This observation is in excellent agreement to the experimental value of ~ 11 water molecules.²⁶ Our simulations suggest that above the LCST, the difference in the number of water molecules per CH_3 group is ~ 2.0 whereas the same near the hydrophilic group is ~ 0.1 . The standard deviations are ~ 0.26 and ~ 0.1 , respectively. This finding suggests that increasing the temperature changes the number of water molecules in the hydrophobic region significantly, but not the water molecules in the hydrophilic region, and that the

Table 3. Number of Water Molecules in First Hydration Shell at both 278 and 310 K (Data Are Averaged over Last 10 ns of Production Run)

system	temperature (K)	water/ CH_3 group	standard deviation	water/ hydrophilic group	standard deviation
3-mer	278	~ 8.6	0.58	~ 3.0	0.45
	310	~ 8.1	0.63	~ 2.8	0.42
5-mer	278	~ 7.8	0.46	~ 2.5	0.3
	310	~ 7.4	0.46	~ 2.5	0.28
10-mer	278	~ 6.8	0.32	~ 2.2	0.17
	310	~ 6.4	0.34	~ 2.0	0.17
30-mer	278	~ 5.9	0.2	~ 1.9	0.08
	310	~ 3.8	0.26	~ 1.8	0.11

structural arrangement of water molecules near hydrophobic groups of PNIPAM is different at 278 K compared with 310 K. The reduced level of hydration above LCST suggests that hydrophobic interactions are dominant. Closer visual analysis of the simulation trajectories indicates that the water cages around the polymer are broken above the LCST. This atomistic picture agrees with previously reported experimental studies that speculate that the hydrophobic collapse is a cooperative process wherein adjacent hydrophobic pockets coalesce via hydrophobic interactions to stabilize the collapsed particle.^{26,27}

To further explore the importance of hydrogen bonding between polymer and water in keeping the polymer hydrophilic, we simulated the 30-mer system with charges biased to reduce the extent of hydrogen bonding. To accomplish this, we turned off the hydrogen bonding between polymer and water by setting the partial charges of hydrophilic atoms ($\text{C}=\text{O}$ and $\text{N}-\text{H}$) to zero. Overall charge on PNIPAM was zero to ensure system neutrality. For this case, we observed the formation of globular phase below and above the LCST at a much shorter time: ~ 700 ps. This finding suggests that hydrogen bonding between polymer and water plays a very important role in maintaining the solvation and keeping the polymer hydrophilic.

c. *Network of Water Molecules between Monomers.* Analysis of the network of water molecules between monomer units can provide useful atomic scale insights into the conformation of water molecules close to the polymer. We observe that the conformation of water close to the polymer is strongly correlated to the polymer chain length and is significantly different depending on the number of monomer units. Figure 8a shows the schematic of hydrogen bonding network formed by water in the first hydration shell for 5-mer below the LCST, namely at 278 K. Figure 8b shows the corresponding simulation snapshot of the equilibrated PNIPAM 5-mer. In the previous section, we note that the average number of water molecules for the 5-mer is ~ 15 – 16 per monomer. Atomic scale distribution of these water molecules around the monomer unit is shown in Figure 8b. Indeed, we observe that each monomer unit is surrounded by ~ 16 water molecules. It can be seen that each carbonyl oxygen of monomer side chain forms a hydrogen bond with hydrogen of two water molecules. The amide group forms hydrogen bond with a single water molecule. Additionally, there is hydrogen bonding between the ~ 16 water molecules. These hydrogen bond bridges between the monomer units play an important role in sustaining an extended conformation of short oligomer PNIPAM at the simulated temperatures (278 and 310 K). Note that short oligomers undergo faster conformational fluctuations compared with longer chains.

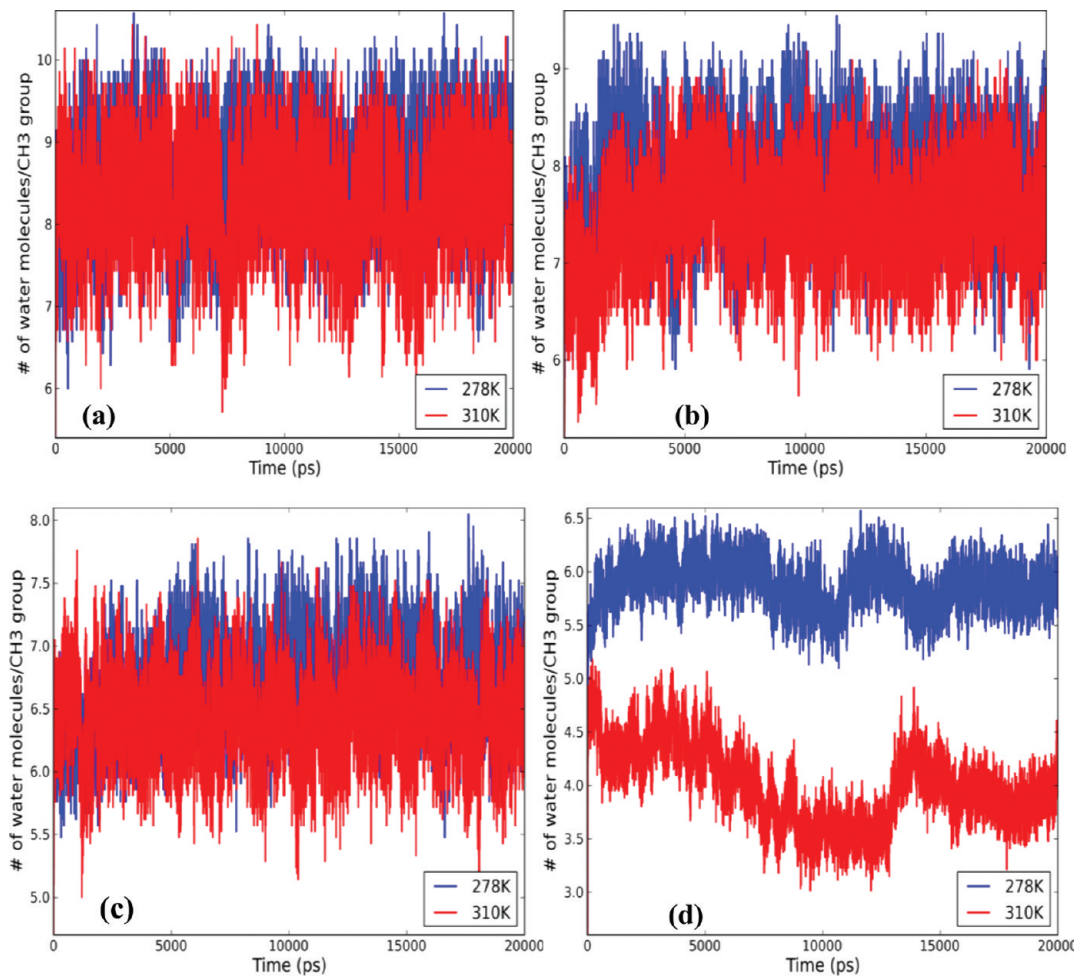


Figure 7. Number of water molecules in first hydration shell near hydrophobic groups: (a) 3-mer, (b) 5-mer, (c) 10-mer, and (d) 30-mer, at both 278 and 310 K.

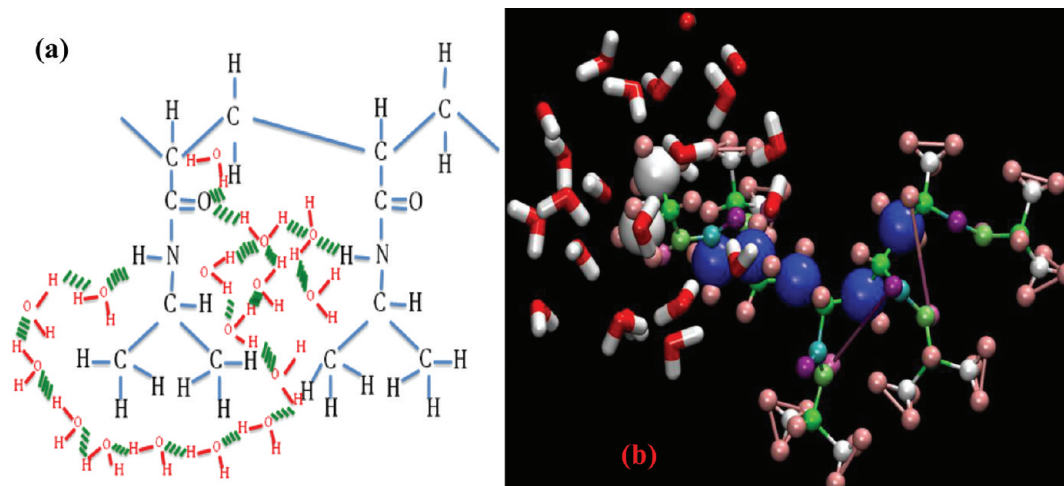


Figure 8. (a) Schematic for hydrogen bond network (hydrogen bond is shown in green color) at 278 K in 5-mer and (b) corresponding snapshot backbone CH₂ shown in blue. Carbon of CH₃ is shown in gray. For the sake of clarity, we only depict a single monomer unit. The arrangement shown in plot a is an approximate 2-D schematic representation of the 3-D arrangement of water molecules around the monomer that are found in our simulations.

Figures 9 and 10 show two possible types of hydrogen bonding network found in this study in 30-mer below the LCST. One of the conformations of the polymer–water network is shown schematically in Figure 9a. Its corresponding atomistic representation obtained from the simulations is

shown in Figure 9b. Two adjacent monomers, in Figure 9b, are shown in orange (referred as monomer A) and green color (referred as monomer B), respectively. Indices 1 and 2 shown in Figure 9b correspond to water molecules forming hydrogen bond with carbonyl oxygen of PNIPAM monomer A. Index 4

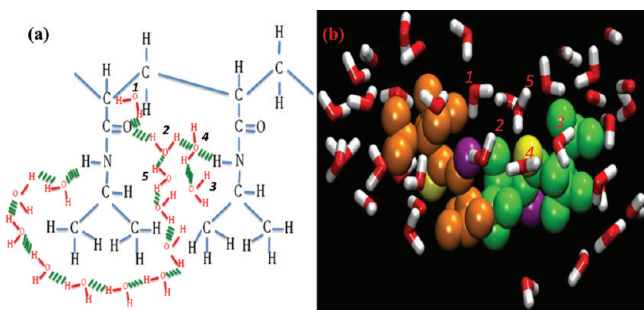


Figure 9. (a) Schematics for hydrogen bond network (hydrogen bond shown in green) at 278 K in two adjacent monomers in 30-mer forming hydrogen bonds and (b) corresponding simulated snapshot showing atomistically the two monomers surrounded by water molecules (carbonyl oxygen and amide nitrogen, shown in purple and yellow, respectively). The arrangement shown in plot a is an approximate 2-D schematic representation of the 3-D arrangement of water molecules around the monomer that are found in our simulations.

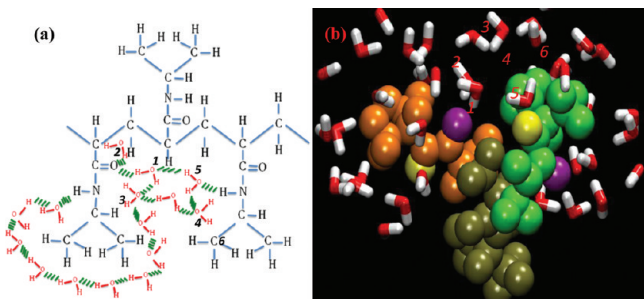


Figure 10. (a) Schematics for hydrogen bond network (hydrogen bond shown in green) at 278 K in two alternate monomers in 30-mer forming hydrogen bonds and (b) corresponding snapshot generated in our atomistic simulation. The 3 adjacent monomers are shown in orange, tan and green (carbonyl oxygen and amide nitrogen shown in purple and yellow, respectively). The arrangement shown in plot a is an approximate 2-D schematic representation of the 3-D arrangement of water molecules around the monomer that are found in our simulations.

represents a water molecule forming hydrogen bond with amide group of PNIPAM side chain of monomer B. Index 3 represents a water molecule which forms hydrogen bond with another water molecule, i.e., index 4 and index 5. Indices 1 through 5 form a compact network comprised of hydrogen

bond bridges between the water in the first hydration and monomers A and B. The simulated network shown schematically in Figure 9a and atomistically in Figure 9b is similar to that identified in the experimental studies of Ono and Shikata.²⁵ Note that this network between two adjacent monomers comprises five water molecules, which is in good agreement with the experimentally reported value in ref 25.

In addition to the conformation shown in Figure 9, we also observe another conformation of water-polymer network (shown in Figure 10). In Figure 10b, the three adjacent monomers A, B, and C are represented by orange, tan, and green, respectively. Figure 10b shows the hydrogen bond network of water molecules with polymer and itself in between two alternate PNIPAM monomers (A and C). Index 1 and 2 represent water molecules forming a hydrogen bond with carbonyl oxygen of monomer A. Index 3 represents a water molecule which forms a hydrogen bond with water molecule, i.e., index 2. Index 4 represents water molecule hydrogen bonded to index 3. Index 5 forms hydrogen bond with the amide group of monomer C. Index 6 is hydrogen bonded to index 5. Together, these water molecules appear to stabilize the solvation cage near the hydrophobic groups. Note that this conformation is different from that shown in Figure 9 since there are six water molecules involved in bridging and stabilizing the alternate monomers in the polymer chain. Interestingly, although this conformation was not identified in the experimental study of Ono and Shikata, they do report the number of water molecules between monomers to be $\sim 5-6$, which is in excellent agreement with our simulations.²⁵

d. Residence Probability Analysis. Figure 11 shows the $P_{\text{res}}(t)$ for water molecules near the hydrophilic groups of PNIPAM below and above the LCST. $P_{\text{res}}(t)$ calculated using the intermittent definition (please see section II.b) allows us to quantify how long on average, one water molecule resides within a distinct hydration layer formed around the polymer. We find that the residence probability depends strongly on the temperature and the length of the PNIPAM chain. $P_{\text{res}}(t)$ increases with an increase in the chain length of PNIPAM. This shows that water molecules in hydrophilic and hydrophobic region of polymer reside for longer times with increase in the chain length (see Supporting Information, Table S2).

The results in Figure 11 further suggest that water molecules in the first hydration layer (within 5.5 Å of carbon atom of CH_3 group polymer side chain) reside near the hydrophilic groups

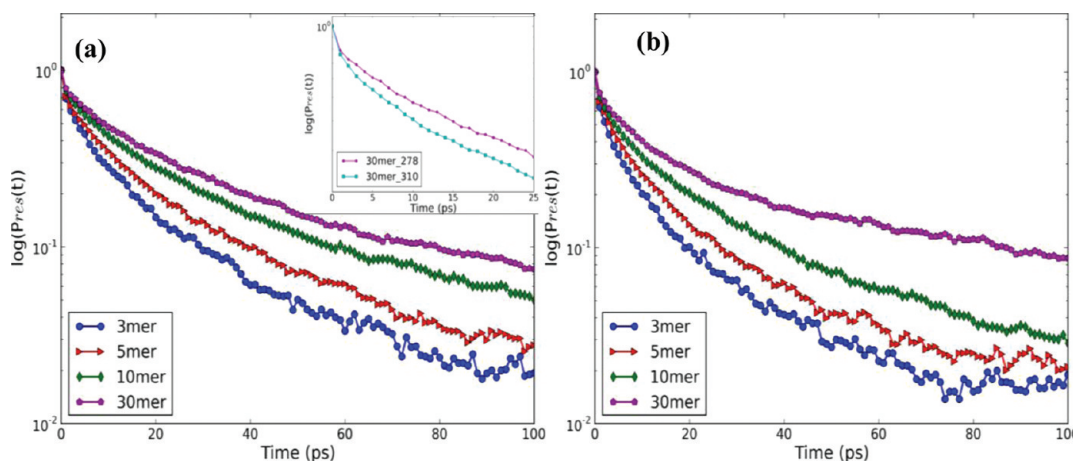


Figure 11. Semilog plot of residence probability of water molecules, by intermittent definition, near hydrophilic region (a) at 278 K and (b) 310 K. Inset shows a plot for 30-mer at 278 and 310 K.

significantly longer for 30-mer than for 3-mer, both below and above the LCST. $P_{\text{res}}(t)$ decreases slowly with increase in the chain length of PNIPAM at both 278 and 310 K. We note that the water molecules in hydration layers farther from the polymer approach the dynamical properties of bulk water.

Comparison of Figure 11a with Figure 11b shows that the residence probability of water molecules for all the simulated systems above the LCST is lower than the residence probability below LCST. When the temperature increases from 278 to 310 K (shown for 30-mer in Figure 11a), we observe that $P_{\text{res}}(t)$ decays faster. The slow dynamical behavior of $P_{\text{res}}(t)$ below LCST, supported by the structural properties of first-layer water molecules previously discussed, indicates energetically stable conformations with pronounced water-polymer correlation. The

slow dynamical behavior of water molecules below the LCST could also be the result of PNIPAM being hydrophilic below LCST, which allows PNIPAM to form strong hydrogen bonds with water molecules. The stronger hydrogen bonding could help bind the water molecules for longer time. This shows that structure of water near polymer, in the case of 30-mer, is more stable below the LCST, namely at 278 K. The stable structure of water molecules might play an important role in keeping the polymer hydrated as well as in keeping the water cage stable. It might be reasonable to assume that this behavior will be followed by longer oligomers/polymers (oligomers with ~ 1000 monomer units).

e. Hydrogen Bonding Lifetimes. Hydrogen bonding characteristics were evaluated using the geometric criteria for

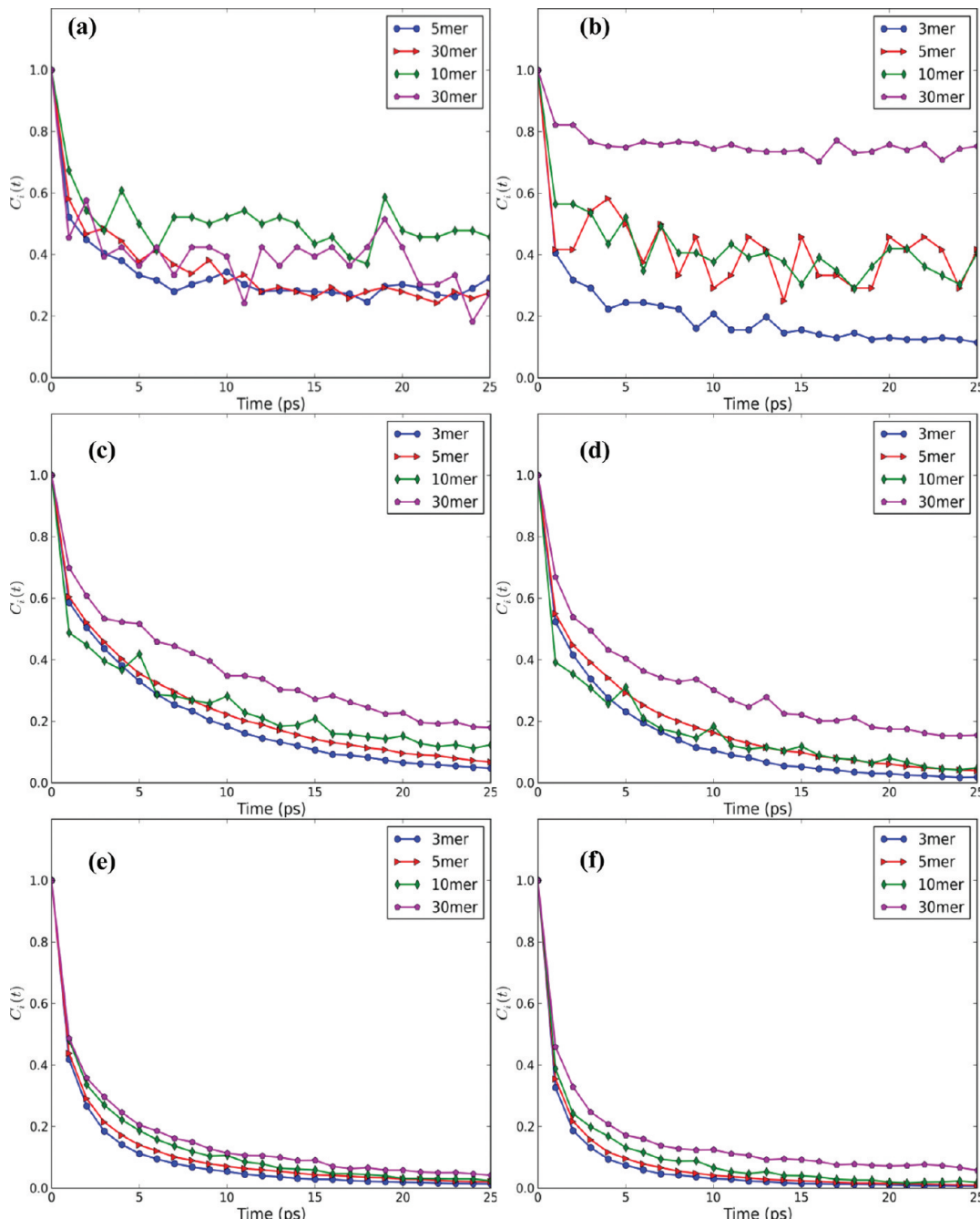


Figure 12. Hydrogen bond correlations for polymer–polymer (type 1), polymer–water (type 2) and water–polymer (type 3) by intermittent definition, at 278 K (a, c, and e) and at 310 K (b, d, and f), respectively.

hydrogen bonding, as described previously in section II.b. In the systems studied, the hydrogen bonds were classified into three types based on donor–acceptor pair: (1) polymer((N–)H)–polymer(O(=C)), (2) polymer((N–)H)–water(O), and (3) water((O–)H)–polymer(O(=C)). The results of these analyses both below and above the LCST, by the definition of intermittent autocorrelation function, are shown in Figure 12a–f. In the case of type 1 hydrogen bonds, the polymer is both the donor and acceptor. As shown in parts a and b of Figure 12, for PNIPAM with 30-mer, the hydrogen bond correlation decays faster at 278 K than at 310 K. In the case of 3-, 5-, and 10-mer, we do not observe any significant change in the hydrogen bond correlations for type 1 hydrogen bonds (see Tables S3, S4, and S5 in the Supporting Information). The slower decay observed in the case of 30-mer at 310 K can be attributed to the globule conformation at 310 K which leads to strong hydrogen bonding in the polymer. Autocorrelation decays more slowly with increasing chain length. This slower decay is due to an increase in the polymer–polymer interactions with increasing chain length. We find a similar behavior in decay characteristics for hydrogen bonds defined by continuous correlation function.

Comparison of type 2 and type 3 interactions, where the polymer is donor and acceptor respectively, suggests that the hydrogen correlation for type 3 (Figure 12e,f) decays faster when compared to hydrogen correlation for type 2 (Figure 12c,d), at both 278 and 310 K. This slower decay dynamic indicates that the hydrogen bond formed between carbonyl oxygen (op) and hydrogen of water (hw) is less stable when compared with the hydrogen bond formed between hydrogen of amide group (N(H)) and water oxygen (ow). Figure 12c,e and Figure 12d,f represent type 2 and type 3 interactions below and above the LCST, respectively. We find that the hydrogen bond correlation decays slowly with increase in the chain length, at both 278 and 310 K. This slow decay indicates that the hydrogen bond network formed between PNIPAM with 30-mer and water and between water and water is more stable than the hydrogen bond network formed between PNIPAM with 3-mer and water and between water and water.

IV. CONCLUSION

Molecular dynamics (MD) simulations of an aqueous solution of Poly(*N*-isopropylacrylamide) (PNIPAM), a thermo-sensitive polymer, were performed to understand the atomic-scale mechanisms behind the conformational changes when the temperature is changed through the lower critical solution temperature (LCST). We have studied size-dependent conformational change of individual PNIPAM chains consisting of 3-, 5-, 10-, and 30-mers in the presence of aqueous media. Simulations were carried out at 278 and 310 K, which is below and above the LCST of PNIPAM. Structural analysis performed using various dynamical correlation functions, such as radius of gyration (R_g) and radial distribution function (RDF), suggests that PNIPAM with a degree of polymerization greater than 30 monomer units undergoes a coil-to-globule transition above the LCST. For short oligomer chains (3-, 5-, and 10-mers), this transition is not clearly observed. The chain length in the case of short oligomers fluctuates around the mean value. PNIPAM consisting of 3-, 5-, and 10-mer did not show a distinct coil-to-globule transition; however, for 30-mer of PNIPAM there exist two distinct temperature-based regimes.

In the case of 30-mer, below LCST (namely, at 278 K), the water molecules in the first hydration layer around hydrophilic

groups arrange themselves in an ordered manner to form hydrogen bonds with the polymer, which results in the hydrophilic interactions being dominant compared to hydrophobic interactions. Above LCST, this arrangement of water is not stable and the hydrophobic interactions become dominant, which contributes to the collapse of the polymer. Around hydrophobic groups of polymer, water forms cage-like structures to form hydrogen bond among them both below and above the LCST, though above the LCST this cage structure is significantly different from the one below LCST.

The structure of solvated water in the first few hydration shells was analyzed by visual examination of the snapshots during simulations and by computing the average number of water molecules in the first hydration shell of polymer for all the chain lengths at 278 and 310 K. We have determined the various stable conformations of water-polymer structure as a function of the polymer chain length. Our analysis of these simulations suggests that the number of water molecules per monomer decreases with the increase in the chain length and with an increase in the temperature. This decrease in the number of water molecules per monomer could be attributed to the slower fluctuation in the mean value of the chain length of PNIPAM consisting of 30-mer compared with PNIPAM consisting of 3-mer. For 30-mer, which shows a coil-to-globule transition above the LCST, the average number of water molecules calculated at 278 K were ~12 in the first hydration shell of PNIPAM, which is close to the experimentally observed value.²⁶ The simulated trajectories were used to quantify the atomistic ordering of water near the polymer. For stable polymer conformations, the number of water molecules forming hydrogen bonding network and involved in the bridging between two adjacent and alternate monomers was found to be 5–6.

Stability of the atomically ordered first hydration shell around the polymer was evaluated by analyzing the residence probability and hydrogen bonding characteristic of PNIPAM in water. Residence probability of water increases with the length of the polymer chain, indicating that water molecules are forming stable cage-like structures in the presence of longer polymer chains. Below the LCST, residence probability correlation function decays slowly as compared with that above the LCST. The faster decay dynamics above the LCST indicates that the increased temperature results in an increased entropy of water molecules which disrupts the cage-like structure. Our simulations thus suggest that the collapse of stable water structure in PNIPAM with 30-mer above the LCST leads to a coil-to-globule transition, a phenomena which is found to be absent in short oligomers like 3-, 5-, and 10-mer.

The hydrogen bonding autocorrelation function indicates that type (1) hydrogen bonding stability in the case of 30-mer increases above the LCST as PNIPAM forms a globule conformation. Hydrogen bonds formed between water and amide group (N(H)) of PNIPAM are more stable than hydrogen bonds between water and carbonyl oxygen (op). In the case of 3-, 5-, and 10-mer, there is no significant difference above the LCST, which explains the lack of a coil-to-globule transformation in the simulated temperature range. Hydrogen bond autocorrelation, for type 2 and type 3, decays slowly with an increase in the chain length of PNIPAM. This suggests that water molecules form more stable conformations in the presence of 30-mer of PNIPAM compared to the 3-, 5-, and 10-mer of PNIPAM.

The dynamics of water solvation and localized ordering around the polymer chains play an important role in determining

the LCST transition. For the various polymer chain lengths simulated here, the solvation dynamics and local structure of water influences the competition between hydrophilic interactions and hydrophobic interactions and therefore dictates the phase transition at LCST. Our study provides insights into the atomistic mechanism of polymer collapse and the role of solvation dynamics in inducing coil-to-globule structural phase transitions in thermo-sensitive polymers through the LCST.

■ ASSOCIATED CONTENT

Supporting Information

Table S1, PCFF parameters for water model; Table S2, decay time for residence probability; Table S3, decay time for hydrogen bond correlation function for polymer–polymer (type 1) hydrogen bonds; Table S4, decay time for hydrogen bond correlation function for polymer–water (type 2) hydrogen bonds; Table S5, decay time for hydrogen bond correlation function for water–polymer (type 3) hydrogen bonds. This material is available free of charge via the Internet at <http://pubs.acs.org>.

■ AUTHOR INFORMATION

Corresponding Author

*E-mail: (S.K.R.S.) skrssank@anl.gov; (D.C.M.) mancini@anl.gov.

Notes

The authors declare no competing financial interest.

■ ACKNOWLEDGMENTS

Use of the Center for Nanoscale Materials was supported by the U.S. Department of Energy, Office of Science, Office of Basic Energy Sciences, under Contract No. DE-AC02-06CH11357.

■ REFERENCES

- (1) Granick, S.; Rubinstein, M. *Nat. Mater.* **2004**, *3*, 586–587.
- (2) Katsumoto, Y.; Tanaka, T.; Sato, H.; Ozaki, Y. *J. Phys. Chem. A* **2002**, *106*, 3429–3435.
- (3) Kamata, K.; Araki, T.; Tanaka, H. *Phys. Rev. Lett.* **2009**, *102*, 108303.
- (4) Blavatska, V.; Janke, W. *Phys. Rev. E* **2009**, *80*, 051805.
- (5) Briber, R. M.; Liu, X.; Bauer, B. J. *Science* **1995**, *268*, 395–397.
- (6) Bajpai, A. K.; Bajpai, J.; Saini, R.; Gupta, R. *Polym. Rev.* **2011**, *51*, 53–97.
- (7) Cheng, H.; Shen, L.; Wu, C. *Macromolecules* **2006**, *39*, 2325–2329.
- (8) Wang, X.; Wu, C. *Macromolecules* **1999**, *32*, 4299–4301.
- (9) Wu, C.; Wang, X. *Phys. Rev. Lett.* **1998**, *80*, 4092–4094.
- (10) Lue, S. J.; Chen, C.-H.; Shih, C.-M. *J. Macromol. Sci., Part B: Phys.* **2011**, *50*, 563–579.
- (11) Kikuchi, A.; Okano, T. *Prog. Polym. Sci.* **2002**, *27*, 1165–1193.
- (12) Liang, D.; Song, L.; Zhou, S.; Zaitsev, V. S.; Chu, B. *Electrophoresis* **1999**, *20*, 2856–2863.
- (13) Ohya, S.; Nakayama, Y.; Matsuda, T. *Biomacromolecules* **2001**, *2*, 856–863.
- (14) Jeong, B.; Kim, S. W.; Bae, Y. H. *Adv. Drug Delivery Rev.* **2001**, *54*, 37–51.
- (15) Choi, C.; Chae, S. Y.; Nah, J.-W. *Polymer* **2006**, *47*, 4571–4580.
- (16) Chung, J. E.; Yokoyama, M.; Yamato, M.; Aoyagi, T.; Sakurai, Y.; Okano, T. *J. Controlled Release* **2002**, *62*, 115–127.
- (17) Shan, J.; Zhao, Y.; Granqvist, N.; Tenhu, H. *Macromolecules* **2009**, *42*, 2696–2701.
- (18) Grabowski, C. A.; Mukhopadhyay, A. *Phys. Rev. Lett.* **2007**, *98*, 207801–207804.
- (19) Schild, H. G. *Prog. Polym. Sci.* **1992**, *17*, 163–249.
- (20) Wang, X.; Qiu, X.; Wu, C. *Macromolecules* **1998**, *31*, 2972–2976.
- (21) Tanaka, N.; Matsukawa, S.; Kurosu, H.; Ando, I. *Polymer* **1998**, *39*, 4703–4706.
- (22) Pamies, R.; Zhu, K.; Kjønksen, A.-L.; Nyström, B. *Polym. Bull.* **2009**, *62*, 487–502.
- (23) Autieri, E.; Chiessi, E.; Lonardi, A.; Paradossi, G.; Sega, M. *J. Phys. Chem. B* **2011**, *115*, 5827–5839.
- (24) Maeda, Y.; Nakamura, T.; Ikeda, I. *Macromolecules* **2001**, *34*, 1391–1399.
- (25) Ono, Y.; Shikata, T. *J. Phys. Chem. B* **2007**, *111*, 1511–1513.
- (26) Ono, Y.; Shikata, T. *J. Am. Chem. Soc.* **2006**, *128*, 10030–10031.
- (27) Shibayama, M.; Morimoto, M.; Nomura, S. *Macromolecules* **1994**, *27*, 5060–5066.
- (28) Tönsing, T.; Oldiges, C. *Phys. Chem. Chem. Phys.* **2001**, *3*, 5542–5549.
- (29) Du, H.; Wickramasinghe, R.; Qian, X. *J. Phys. Chem.* **2010**, *114*, 16594–16604.
- (30) Deshmukh, S.; Mooney, D. A.; McDermott, T.; Kulkarni, S.; MacElroy, J. M. D. *Soft Matter* **2009**, *5*, 1514–1521.
- (31) Tamai, Y.; Tanaka, H. *Macromolecules* **1996**, *29*, 6761–6769.
- (32) Tamai, Y.; Tanaka, H. *Macromolecules* **1996**, *29*, 6750–6760.
- (33) Lele, A. K.; Hirve, M. M.; Badiger, M. V.; Mashelkar, R. A. *Macromolecules* **1997**, *30*, 157–159.
- (34) Cho, E. C.; Lee, J.; Cho, K. *Macromolecules* **2003**, *36*, 9929–9934.
- (35) Chiessi, E.; Lonardi, A.; Paradossi, G. *J. Phys. Chem.* **2010**, *114*, 8301–8312.
- (36) Gangemi, F.; Longhi, G.; Abbate, S.; Lebon, F.; Cordone, R.; Ghilardi, G. P.; Fornili, S. L. *J. Phys. Chem. B* **2008**, *112*, 11896–11906.
- (37) Longhi, G.; Lebon, F.; Abbate, S.; Fornili, S. L. *Chem. Phys. Lett.* **2004**, *386*, 123–127.
- (38) Raos, G.; Allegra, G.; Ganazzoli, F. *J. Chem. Phys.* **1994**, *100*, 7804–7813.
- (39) Ostrovsky, B.; Bar-Yam, Y. *Comput. Polym. Sci.* **1993**, *3*, 9–13.
- (40) Tanaka, G.; Mattice, W. L. *Macromolecules* **1995**, *28*, 1049–1059.
- (41) Ahmed, Z.; Gooding, E.; Pimenov, K.; Wang, L.; Asher, S. *J. Phys. Chem. B* **2009**, *113*, 4248–4256.
- (42) Pang, J.; Yang, H.; Cheng, R. *J. Phys. Chem. B* **2010**, *114*, 7429–7438.
- (43) Du, H.; Qian, X. *J. Polym. Sci., Part B: Polym. Phys.* **2011**, *49*, 1112–1122.
- (44) Ray, B.; Okamoto, Y.; Kamigaito, M.; Sawamoto, M.; Seno, K.-i.; Kanaoka, S.; Aoshima, S. *Polym. J.* **2005**, *37*, 234–237.
- (45) Tanaka, F.; Koga, T. *Phys. Rev. Lett.* **2008**, *101*, 028302–4.
- (46) Yasushi, M.; Tomoya, N.; Isao, I. *Macromolecules* **2002**, *35*, 10172–10177.
- (47) Li, I. T. S.; Walker, G. C. *J. Am. Chem. Soc.* **2010**, *132*, 6530–6540.
- (48) Kojima, H.; Tanaka, F. *Macromolecules* **2010**, *43*, 5103–5113.
- (49) Sun, S.; Hu, J.; Tang, H.; Wu, P. *J. Phys. Chem. B* **2010**, *114*, 9761–9770.
- (50) Sun, H. *Macromolecules* **1995**, *28*, 701–712.
- (51) Sun, H.; Mumby, S.; Maple, J.; Hagler, A. *J. Am. Chem. Soc.* **1994**, *116*, 2978–2987.
- (52) Fan, H. B.; Yuen, M. M. F. *Polymer* **2007**, *48*, 2174–2178.
- (53) Patnaik, S. S.; Pachter, R. *Polymer* **1999**, *40*, 6507–6519.
- (54) Fritz, L.; Hofmann, D. *Polymer* **1997**, *38*, 1035–1045.
- (55) Maple, J. R.; Thacher, T. S.; Dinur, U.; Hagler, A. T. *Chem. Des. Automation News* **1990**, *5*.
- (56) Sun, H. *J. Comput. Chem.* **1994**, *15*, 752–768.
- (57) Knopp, B.; Suter, U. W.; Gusev, A. A. *Macromolecules* **1997**, *30*, 6107–6113.
- (58) Allen, M. P.; Tildesley, D. J. *Computer Simulations of Liquid*; Clarendon Press: Oxford, U.K., 1987.
- (59) Plimpton, S. J. *Comput. Phys.* **1995**, *117*, 1–19.
- (60) Luzar, A.; Chandler, D. *J. Chem. Phys.* **1993**, *98*, 8160–8173.
- (61) Ladanyi, B. M.; Skaf, M. S. *Annu. Rev. Phys. Chem.* **1993**, *44*, 335–368.
- (62) Rapaport, D. C. *Mol. Phys.* **1983**, *50*, 1151–1162.
- (63) Duffy, D. M.; Rodger, P. M. *J. Am. Chem. Soc.* **2002**, *124*, 5206–5212.